Spin dynamics in the pressure-induced two-leg ladder cuprate superconductor $Sr_{14-x}Ca_xCu_{24}O_{41}$

Jihong Qin
Department of Physics, University of Science and Technology Beijing, Beijing 100083, China

Yu Lan
Department of Physics, Jinan University, Guangzhou 510632, China

Shiping Feng
Department of Physics, Beijing Normal University, Beijing 100875, China

Within the two-leg t-J ladder, the spin dynamics of the pressure-induced two-leg ladder cuprate superconductor $Sr_{14-x}Ca_xCu_{24}O_{41}$ is studied based on the kinetic energy driven superconducting mechanism. It is shown that in the pressure-induced superconducting state, the incommensurate spin correlation appears in the underpressure regime, while the commensurate spin fluctuation emerges in the optimal pressure and overpressure regimes. In particular, the spin-lattice relaxation time is dominated by a temperature linear dependence term at low temperature followed by a peak developed below the superconducting transition temperature, in qualitative agreement with the experimental observation on $Sr_{14-x}Ca_xCu_{24}O_{41}$.

PACS numbers: 74.25.nj, 74.25.Ha, 74.20.Mn, 74.62.Fj

The doped two-leg ladder cuprate $Sr_{14-x}Ca_xCu_{24}O_{41}$ is a system in which a superconducting (SC) state is realized by applying a high pressure of 3 $\sim$ 8GPa in the highly charge carrier doped region[1]. This pressure-induced superconductor possesses a complex structure consisting of the Cu_2O_3 two-leg ladder and CuO_2 chain[2,3], then charge carriers are transferred from CuO_2 chain unit by substituting Ca for Sr. At the half-filling, the ground state is a spin liquid state with a finite spin gap[4] and this gapped spin liquid state persists even in the highly charge carrier doped region[5]. Moreover, the structure of $Sr_{14-x}Ca_xCu_{24}O_{41}$ under high pressure remains the same as the case in ambient pressure[6], and then the spin background in the SC phase does not drastically alter its spin gap properties[7]. Experimentally, by virtue of systematic studies using the nuclear magnetic resonance (NMR) and nuclear quadrupole resonance (NQR), the dynamical spin response of $Sr_{14-x}Ca_xCu_{24}O_{41}$ has been well established now[8–10]. In the pressure-induced SC state, the pressure promotes the existence of low-lying spin excitations giving rise to a residual spin susceptibility at low temperature[9]. Furthermore, the spin-lattice relaxation time is dominated by a temperature linear dependence term at low temperature followed by a peak developed below the SC transition temperature[8]. In this case, the interplay between the magnetic excitation and superconductivity in two-leg ladder cuprate superconductors is of central concern as is the case with the planar cuprate superconductors[11].

In our earlier work[12] using the charge-spin separation (CSS) fermion-spin theory[13,14], the dynamical spin response of $Sr_{14-x}Ca_xCu_{24}O_{41}$ in the *normal state* has been studied, where our calculations clearly demonstrate a crossover from the incommensurate antiferromagnetism in the weak interchain coupling regime to commensurate spin fluctuation in the strong interchain coupling regime. In particular, the nuclear spin-lattice relaxation time decreases exponentially with decreasing temperatures[5,15]. Furthermore, within the kinetic energy driven SC mechanism[16], we have discussed the pressure-induced superconductivity[17] in $Sr_{14-x}Ca_xCu_{24}O_{41}$, and the result of the pressure dependence of the SC transition temperature is in good agreement with the corresponding experimental data of $Sr_{14-x}Ca_xCu_{24}O_{41}$[6]. However, in the pressure-induced SC state, a microscopic study of the dynamical spin response of $Sr_{14-x}Ca_xCu_{24}O_{41}$ has not been performed theoretically thus far although the dynamical spin response has been measured experimentally. In this paper, we study the spin dynamics of $Sr_{14-x}Ca_xCu_{24}O_{41}$ in the pressure-induced SC state within the kinetic energy driven SC mechanism, where we calculate the dynamical spin structure factor, and then reproduce qualitatively some main features of the corresponding temperature dependence of the spin-lattice relaxation time in $Sr_{14-x}Ca_xCu_{24}O_{41}$.

The basic element of the two-leg ladder cuprates is the two-leg ladder, which is defined as two parallel chains of ions, while the coupling between the two chains that participates in this structure is through rungs[2,3]. It has been shown[7] from the experiments that the ratio of the interladder resistivity to in-ladder resistivity is $R=\rho_a(T)/\rho_c(T)\sim 10$, this large magnitude of the resistivity anisotropy reflects that the interladder mean free path is shorter than the interladder distance, and the charge carriers are tightly confined to the ladders, therefore the common two-leg ladders in the doped two-leg ladder cuprates clearly dominate the most physical properties. In this case, it has been argued that the essential physics of the doped two-leg ladder cuprates can be de-

scribed by the t-J ladder as[18],

$$\begin{aligned} H &= -t_{\parallel}\sum_{i\hat{\eta}a\sigma}C^{\dagger}_{ia\sigma}C_{i+\hat{\eta}a\sigma} - t_{\perp}\sum_{i\sigma}(C^{\dagger}_{i1\sigma}C_{i2\sigma} + \mathrm{H.c.}) \\ &- \mu\sum_{ia\sigma}C^{\dagger}_{ia\sigma}C_{ia\sigma} \\ &+ J_{\parallel}\sum_{i\hat{\eta}a}\mathbf{S}_{ia}\cdot\mathbf{S}_{i+\hat{\eta}a} + J_{\perp}\sum_{i}\mathbf{S}_{i1}\cdot\mathbf{S}_{i2}, \end{aligned} \quad (1)$$

supplemented by the local constraint $\sum_{\sigma}C^{\dagger}_{ia\sigma}C_{ia\sigma}\leq 1$ to remove double occupancy, where $\hat{\eta}=\pm\hat{x}$, i runs over all rungs, $\sigma(=\uparrow,\downarrow)$ and $a(=1,2)$ are spin and leg indices, respectively, $C^{\dagger}_{ia\sigma}$ ($C_{ia\sigma}$) are the electron creation (annihilation) operators, $\mathbf{S}_{ia}=(S^{x}_{ia},S^{y}_{ia},S^{z}_{ia})$ are the spin operators, and μ is the chemical potential. This local constraint can be treated properly in analytical calculations within the CSS fermion-spin theory[13,14], $C_{ia\uparrow}=h^{\dagger}_{ia\uparrow}S^{-}_{ia}$ and $C_{ia\downarrow}=h^{\dagger}_{ia\downarrow}S^{+}_{ia}$, where the spinful fermion operator $h_{ia\sigma}=e^{-i\Phi_{i\sigma}}h_{ia}$ describes the charge degree of freedom together with some effects of the spin configuration rearrangements due to the presence of the doped charge carrier itself, while the spin operator S_{ia} describes the spin degree of freedom, then the electron local constraint for the single occupancy, $\sum_{\sigma}C^{\dagger}_{ia\sigma}C_{ia\sigma}=S^{+}_{ia}h_{ia\uparrow}h^{\dagger}_{ia\uparrow}S^{-}_{ia}+S^{-}_{ia}h_{ia\downarrow}h^{\dagger}_{ia\downarrow}S^{+}_{ia}=h_{ia}h^{\dagger}_{ia}(S^{+}_{ia}S^{-}_{ia}+S^{-}_{ia}S^{+}_{ia})=1-h^{\dagger}_{ia}h_{ia}\leq 1$, is satisfied in analytical calculations. Although in common sense $h_{ia\sigma}$ is not a real spinful fermion operator, it behaves like a spinful fermion. This is followed from a fact that the spinless fermion h_{ia} and spin operators S^{+}_{ia} and S^{-}_{ia} obey the anticommutation relation and Pauli spin algebra, respectively, it is then easy to show that the spinful fermion $h_{ia\sigma}$ also obey the same anticommutation relation as the spinless fermion h_{ia}. In particular, it has been shown that under the decoupling scheme, this CSS fermion-spin representation is a natural representation of the constrained electron defined in the restricted Hilbert space without double electron occupancy[14]. Moreover, these charge carrier and spin are gauge invariant[13,14], and in this sense, they are real and can be interpreted as the physical excitations[19]. In this CSS fermion-spin representation, the low-energy behavior of the t-J ladder Hamiltonian (1) can be expressed as,

$$\begin{aligned} H &= t_{\parallel}\sum_{i\hat{\eta}a}(h^{\dagger}_{i+\hat{\eta}a\uparrow}h_{ia\uparrow}S^{+}_{ia}S^{-}_{i+\hat{\eta}a}+h^{\dagger}_{i+\hat{\eta}a\downarrow}h_{ia\downarrow}S^{-}_{ia}S^{+}_{i+\hat{\eta}a}) \\ &+ t_{\perp}\sum_{i}(h^{\dagger}_{i2\uparrow}h_{i1\uparrow}S^{+}_{i1}S^{-}_{i2}+h^{\dagger}_{i1\uparrow}h_{i2\uparrow}S^{+}_{i2}S^{-}_{i1} \\ &+ h^{\dagger}_{i2\downarrow}h_{i1\downarrow}S^{-}_{i1}S^{+}_{i2}+h^{\dagger}_{i1\downarrow}h_{i2\downarrow}S^{-}_{i2}S^{+}_{i1}) \\ &+ \mu\sum_{ia\sigma}h^{\dagger}_{ia\sigma}h_{ia\sigma} \\ &+ J_{\parallel\mathrm{eff}}\sum_{i\hat{\eta}a}\mathbf{S}_{ia}\cdot\mathbf{S}_{i+\hat{\eta}a}+J_{\perp\mathrm{eff}}\sum_{i}\mathbf{S}_{i1}\cdot\mathbf{S}_{i2}, \end{aligned} \quad (2)$$

where $J_{\parallel\mathrm{eff}}=J_{\parallel}(1-p)^{2}$, $J_{\perp\mathrm{eff}}=J_{\perp}(1-p)^{2}$, and $p=\langle h^{\dagger}_{ia\sigma}h_{ia\sigma}\rangle=\langle h^{\dagger}_{ia}h_{ia}\rangle$ is the charge carrier doping concentration. Although the CSS fermion-spin representation is a natural representation for the constrained electron under the decoupling scheme[14], so long as $h^{\dagger}_{ia}h_{ia}=1$, $\sum_{\sigma}C^{\dagger}_{ia\sigma}C_{ia\sigma}=0$, no matter what the values of $S^{+}_{ia}S^{-}_{ia}$ and $S^{-}_{ia}S^{+}_{ia}$ are, therefore it means that a *spin* even to an empty site has been assigned. Obviously, this insignificant defect is originated from the decoupling approximation. It has been shown[20] that this defect can be cured by introducing a projection operator P_{i}, i.e., the electron operator $C_{ia\sigma}$ with the single occupancy local constraint can be mapped exactly using the CSS fermion-spin transformation defined with an additional projection operator P_{i}. However, this projection operator is cumbersome to handle in the many cases, and it has been dropped in the actual calculations[12–14,16,17]. It has been shown[13,14,20,21] that such treatment leads to errors of the order p in counting the number of spin states, which is negligible for small dopings. Moreover, the electron single occupancy local constraint still is exactly obeyed even in the mean-field (MF) approximation. These are why the theoretical results[12,17] obtained from the t-J ladder model (2) based on the CSS fermion-spin theory are in qualitative agreement with the experimental observation on the doped two-leg ladder cuprates.

It has been shown from the experiments[1,6,22] that the pressure-induced SC state in the doped two-leg ladder cuprate $Sr_{14-x}Ca_{x}Cu_{24}O_{41}$ is also characterized by the electron Cooper pairs as in the conventional superconductors[23], forming SC quasiparticles. However, because there are two coupled t-J chains in the pressure-induced two-leg ladder cuprate superconductors, the energy spectrum has two branches, and therefore the one-particle spin Green's function, the charge carrier normal and anomalous Green's functions are matrices, and can be expressed as, $D(i-j,\tau-\tau')=D_{L}(i-j,\tau-\tau')+\sigma_{x}D_{T}(i-j,\tau-\tau')$, $g(i-j,\tau-\tau')=g_{L}(i-j,\tau-\tau')+\sigma_{x}g_{T}(i-j,\tau-\tau')$, $\Gamma^{\dagger}(i-j,\tau-\tau')=\Gamma^{\dagger}_{L}(i-j,\tau-\tau')+\sigma_{x}\Gamma^{\dagger}_{T}(i-j,\tau-\tau')$, respectively, where the corresponding longitudinal and transverse parts are defined as $D_{L}(i-j,\tau-\tau')=-\langle T_{\tau}S^{+}_{ia}(\tau)S^{-}_{ja}(\tau')\rangle$, $g_{L}(i-j,\tau-\tau')=-\langle T_{\tau}h_{ia\sigma}(\tau)h^{\dagger}_{ja\sigma}(\tau')\rangle$, $\Gamma^{\dagger}_{L}(i-j,\tau-\tau')=-\langle T_{\tau}h_{ia\uparrow}(\tau)h^{\dagger}_{ja\downarrow}(\tau')\rangle$, and $D_{T}(i-j,\tau-\tau')=-\langle T_{\tau}S^{+}_{ia}(\tau)S^{-}_{ja'}(\tau')\rangle$, $g_{T}(i-j,\tau-\tau')=-\langle T_{\tau}h_{ia\sigma}(\tau)h^{\dagger}_{ja'\sigma}(\tau')\rangle$, $\Gamma^{\dagger}_{T}(i-j,\tau-\tau')=-\langle T_{\tau}h_{ia\uparrow}(\tau)h^{\dagger}_{ja'\downarrow}(\tau')\rangle$, with $a'\neq a$. In this case, the order parameters for the electron Cooper pair also is a matrix $\Delta=\Delta_{L}+\sigma_{x}\Delta_{T}$, with the longitudinal and transverse SC order parameters are defined as,

$$\begin{aligned} \Delta_{L} &= \langle C^{\dagger}_{ia\uparrow}C^{\dagger}_{i+\hat{\eta}a\downarrow}-C^{\dagger}_{ia\downarrow}C^{\dagger}_{i+\hat{\eta}a\uparrow}\rangle=\langle h_{ia\uparrow}h_{i+\hat{\eta}a\downarrow}S^{+}_{ia}S^{-}_{i+\hat{\eta}a} \\ &- h_{ia\downarrow}h_{i+\hat{\eta}a\uparrow}S^{-}_{ia}S^{+}_{i+\hat{\eta}a}\rangle=-\chi_{\parallel}\Delta_{hL}, \end{aligned} \quad (3a)$$

$$\begin{aligned} \Delta_{T} &= \langle C^{\dagger}_{i1\uparrow}C^{\dagger}_{i2\downarrow}-C^{\dagger}_{i1\downarrow}C^{\dagger}_{i2\uparrow}\rangle=\langle h_{i1\uparrow}h_{i2\downarrow}S^{+}_{i1}S^{-}_{i2} \\ &- h_{i1\downarrow}h_{i2\uparrow}S^{-}_{i1}S^{+}_{i2}\rangle=-\chi_{\perp}\Delta_{hT}, \end{aligned} \quad (3b)$$

respectively, where the spin correlation functions $\chi_{\parallel}=\langle S^{+}_{ia}S^{-}_{i+\hat{\eta}a}\rangle$ and $\chi_{\perp}=\langle S^{+}_{i1}S^{-}_{i2}\rangle$, and the longitudinal and

transverse charge carrier pairing order parameters are expressed as $\Delta_{hL} = \langle h_{j a\downarrow} h_{i a\uparrow} - h_{j a\uparrow} h_{i a\downarrow}\rangle$ and $\Delta_{hT} = \langle h_{i2\downarrow} h_{i1\uparrow} - h_{i2\uparrow} h_{i1\downarrow}\rangle$, respectively.

At ambient pressure, the exchange coupling $J_{\parallel}$ along the legs is greater than exchange coupling $J_{\perp}$ across a rung, i.e., $J_{\parallel} > J_{\perp}$, and similarly the hopping $t_{\parallel}$ along the legs is greater than the rung hopping strength $t_{\perp}$, i.e., $t_{\parallel} > t_{\perp}$. In this case, the doped two-leg ladder cuprate $Sr_{14-x}Ca_xCu_{24}O_{41}$ is highly anisotropic material[4,7,15]. However, pressure for realizing superconductivity in doped two-leg ladder cuprates plays a role of stabilizing the metallic state and suppressing anisotropy within the ladders. This is followed an experimental fact[1,6,8,22,24,25] that the distance between ladders and chains is reduced with increasing pressure, and then the coupling between ladders and chains is enhanced. This leads to that the values of $J_{\perp}/J_{\parallel}$ and $t_{\perp}/t_{\parallel}$ increase with increasing pressure. In other words, the pressurization induces anisotropy shrinkage on doped two-leg ladder cuprates, and then there is a tendency toward the isotropy for doped two-leg ladders[1,6,8,22,24,25]. These experimental results explicitly imply that the values of $J_{\perp}/J_{\parallel}$ and $t_{\perp}/t_{\parallel}$ of doped two-leg ladder cuprates are closely related to the pressurization, and therefore the pressure effects can be imitated by a variation of the values of $J_{\perp}/J_{\parallel}$ and $t_{\perp}/t_{\parallel}$. On the other hand, as we have mentioned above, the structure of $Sr_{14-x}Ca_xCu_{24}O_{41}$ by applying a high pressure of $3 \sim 8$GPa remains the same as the case in ambient pressure[6], and then the spin background in the SC phase does not drastically alter its spin gap properties[7]. In this case, the pressure-induced superconductivity in $Sr_{14-x}Ca_xCu_{24}O_{41}$ has been discussed[17] within the kinetic energy driven SC mechanism[16], and a dome-shaped SC transition temperature T_c versus pressure curve is obtained, where the variation of $(t_{\perp}/t_{\parallel})^2$ under the pressure is chosen the same as that of $J_{\perp}/J_{\parallel}$, i.e., $(t_{\perp}/t_{\parallel})^2 = J_{\perp}/J_{\parallel}$. For the convenience in the following discussions, this result of the dome-shaped SC transition temperature T_c versus pressure is replotted in Fig. 1 in comparison with the corresponding experimental result[6] of $Sr_{14-x}Ca_xCu_{24}O_{41}$ (inset), where the maximal SC transition temperature occurs around the optimal pressure ($t_{\perp}/t_{\parallel} \approx 0.7$), then decreases in both underpressure ($t_{\perp}/t_{\parallel} < 0.7$) and overpressure ($t_{\perp}/t_{\parallel} > 0.7$) regimes, and is in good agreement with the corresponding experimental data of $Sr_{14-x}Ca_xCu_{24}O_{41}$[6].

Following our previous discussions[17,26], the longitudinal and transverse parts of the charge carrier normal and anomalous Green functions of the pressure-induced two-leg ladder cuprate superconductors can be obtained as,

$$g_L(k,\omega) = \frac{1}{2}\sum_{\nu=1,2} Z^{(\nu)}_{FA}\left(\frac{U^2_{\nu k}}{\omega - E_{\nu k}} + \frac{V^2_{\nu k}}{\omega + E_{\nu k}}\right), \tag{4a}$$

$$g_T(k,\omega) = \frac{1}{2}\sum_{\nu=1,2} (-1)^{\nu+1} Z^{(\nu)}_{FA}\left(\frac{U^2_{\nu k}}{\omega - E_{\nu k}} + \frac{V^2_{\nu k}}{\omega + E_{\nu k}}\right), \tag{4b}$$

$$\Gamma^{\dagger}_L(k,\omega) = -\frac{1}{2}\sum_{\nu=1,2} Z^{(\nu)}_{FA}\frac{\bar{\Delta}^{(\nu)}_{hz}(k)}{2E_{\nu k}}\left(\frac{1}{\omega - E_{\nu k}} - \frac{1}{\omega + E_{\nu k}}\right), \tag{4c}$$

$$\Gamma^{\dagger}_T(k,\omega) = -\frac{1}{2}\sum_{\nu=1,2} (-1)^{\nu+1} Z^{(\nu)}_{FA}\frac{\bar{\Delta}^{(\nu)}_{hz}(k)}{2E_{\nu k}}\left(\frac{1}{\omega - E_{\nu k}} - \frac{1}{\omega + E_{\nu k}}\right), \tag{4d}$$

where $Z^{(1)-1}_{FA} = Z^{-1}_{F1} - Z^{-1}_{F2}$ and $Z^{(2)-1}_{FA} = Z^{-1}_{F1} + Z^{-1}_{F2}$ with the charge carrier longitudinal and transverse quasiparticle coherent weights Z_{F1} and Z_{F2}, respectively, the charge carrier quasiparticle coherence factors $U^2_{\nu k} = [1+\bar{\xi}_{\nu k}/E_{\nu k}]/2$ and $V^2_{\nu k} = [1-\bar{\xi}_{\nu k}/E_{\nu k}]/2$, the renormalized charge carrier excitation spectrum $\bar{\xi}_{\nu k} = Z^{(\nu)}_{FA}\xi_{\nu k}$, with the MF charge carrier excitation spectrum $\xi_{\nu k} = 2t_{\parallel}\chi_{\parallel}\cos k + \mu + \chi_{\perp}t_{\perp}(-1)^{\nu+1}$, the renormalized charge carrier pair gap function $\bar{\Delta}^{(\nu)}_{hz}(k) = Z^{(\nu)}_{FA}[2\bar{\Delta}_{hL}\cos k + (-1)^{\nu+1}\bar{\Delta}_{hT}]$, and the charge carrier quasiparticle dispersion $E_{\nu k} = \sqrt{[\bar{\xi}_{\nu k}]^2 + \mid \bar{\Delta}^{(\nu)}_{hz}(k)\mid^2}$. While the longitudinal and transverse parts of the MF spin Green's function $D^{(0)}(k,\omega)$ can be obtained as[12],

$$D^{(0)}_L(k,\omega) = \frac{1}{2}\sum_{\mu=1,2}\frac{B_{\mu k}}{\omega^2 - \omega^2_{\mu k}}, \tag{5a}$$

$$D^{(0)}_T(k,\omega) = \frac{1}{2}\sum_{\mu=1,2}(-1)^{\mu+1}\frac{B_{\mu k}}{\omega^2 - \omega^2_{\mu k}}, \tag{5b}$$

where $B_{\mu k} = \lambda[A_1\cos k - A_2] - J_{\perp\rm eff}[\chi_{\perp} + 2\chi^z_{\perp}(-1)^{\mu}][\epsilon_{\perp} + (-1)^{\mu}]$, $\lambda = 4J_{\parallel\rm eff}$, $A_1 = 2\epsilon_{\parallel}\chi^z_{\parallel} + \chi_{\parallel}$, $A_2 = \epsilon_{\parallel}\chi_{\parallel} + 2\chi^z_{\parallel}$, $\epsilon_{\parallel} = 1 + 2t_{\parallel}\phi_{\parallel}/J_{\parallel\rm eff}$, and $\epsilon_{\perp} = 1 + 4t_{\perp}\phi_{\perp}/J_{\perp\rm eff}$, with the spin correlation functions $\chi^z_{\parallel} = \langle S^z_{ia}S^z_{i+\hat{\eta}a}\rangle$, $\chi^z_{\perp} = \langle S^z_{i1}S^z_{i2}\rangle$, the charge carrier particle-hole order parameters $\phi_{\parallel} = \langle h^{\dagger}_{ia\sigma}h_{i+\hat{\eta}a\sigma}\rangle$, $\phi_{\perp} = \langle h^{\dagger}_{i1\sigma}h_{i2\sigma}\rangle$. The

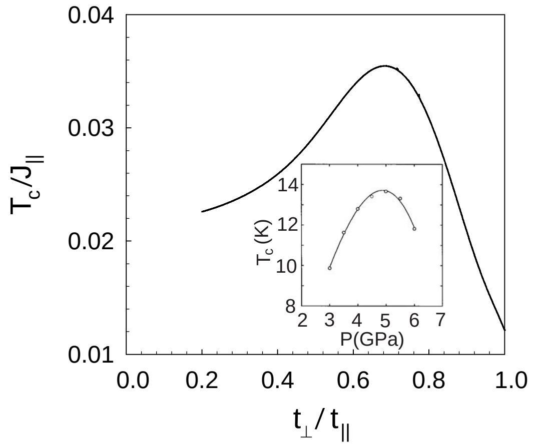

FIG. 1: The superconducting transition temperature as a function of $t_\perp/t_\|$ for $t_\|/J_\| = 2.5$ at $p = 0.25$. Inset: the experimental result of $Sr_{14-x}Ca_xCu_{24}O_{41}$ taken from Ref.[6].

MF spin excitation spectra, $\omega^2_{\mu\mathbf{k}} = \alpha\epsilon_\|\lambda^2 A_1\cos^2k/2 + [X_1 + X_2(-1)^{\mu+1}]\cos k + X_3 + X_4(-1)^{\mu+1}$, where $X_1 = -\epsilon_\|\lambda^2[(\alpha A_2 + 2A_4)/4 + A_3] - \alpha\lambda J_{\perp\rm eff}[\epsilon_\|(C^z_\perp + \chi^z_\perp) + \epsilon_\perp(C_\perp + \epsilon_\|\chi_\perp)/2]$, $X_2 = \alpha\lambda J_{\perp\rm eff}[(\epsilon_\perp\chi_\| + \epsilon_\|\chi_\perp)/2 + \epsilon_\|\epsilon_\perp(\chi^z_\perp + \chi^z_\|)]$, $X_3 = \lambda^2[A_3 - \alpha\epsilon_\| A_1/4 + \epsilon^2_\| A_4/2] + \alpha\lambda J_{\perp\rm eff}[\epsilon_\|\epsilon_\perp C_\perp + 2C^z_\perp] + J^2_{\perp\rm eff}(\epsilon^2_\perp + 1)/4$, $X_4 = -\alpha\lambda J_{\perp\rm eff}[\epsilon_\|\epsilon_\perp\chi_\|/2 + \epsilon_\perp(\chi^z_\| + C^z_\perp) + \epsilon_\| C_\perp/2] - \epsilon_\perp J^2_{\perp\rm eff}/2$, with $A_3 = \alpha C^z_\| + (1-\alpha)/8$, $A_4 = \alpha C_\| + (1-\alpha)/4$, and the spin correlation functions $C_\| = \sum_{\hat{\eta}\hat{\eta}'}\langle S^+_{i+\hat{\eta}a}S^-_{i+\hat{\eta}'a}\rangle/4$, $C^z_\| = \sum_{\hat{\eta}\hat{\eta}'}\langle S^z_{i+\hat{\eta}a}S^z_{i+\hat{\eta}'a}\rangle/4$, $C_\perp = \sum_{\hat{\eta}}\langle S^+_{i2}S^-_{i+\hat{\eta}1}\rangle/2$, and $C^z_\perp = \sum_{\hat{\eta}}\langle S^z_{i1}S^z_{i+\hat{\eta}2}\rangle/2$. In order to satisfy the sum rule for the correlation function $\langle S^+_{ia}S^-_{ia}\rangle = 1/2$ in the absence of the antiferromagnetic (AF) long-range-order, a decoupling parameter α has been introduced in the MF calculation, which can be regarded as the vertex correction[12,17], then all these MF order parameters, decoupling parameter, chemical potential, charge carrier longitudinal and transverse quasiparticle coherent weights Z_{F1} and Z_{F2}, and longitudinal and transverse charge carrier pair gap parameters $\bar{\Delta}_{hL}$ and $\bar{\Delta}_{hT}$ are determined by the self-consistent calculation[17,26].

In the CSS fermion-spin theory[13,14], the AF fluctuation is dominated by the scattering of the spins. In the normal state, the spins move in the charge carrier background, therefore the spin self-energy (then full spin Green's function) in the normal state has been obtained in terms of the collective mode in the charge carrier particle-hole channel[12]. With the help of this full spin Green's function in the normal state, the dynamical spin response of $Sr_{14-x}Ca_xCu_{24}O_{41}$ in the normal state has been discussed[12], and the results are consistent with the corresponding experimental results[5,15]. However, in the present pressure-induced SC state, the spins move in the charge carrier pairing background. On the other hand, we[27] have discussed the optical and transport properties of the doped two-leg ladder cuprates in the underdoped and optimally doped regimes by considering the fluctuations around the MF solution, where the dominant dynamical effect is due to the strong interaction between the charge carriers and spins in the t-J ladder Hamiltonian (2). We believe that this strong interaction between the charge carriers and spins also will dominate the spin dynamics within the same doping regimes. In this case, we can calculate the spin self-energy (then the full spin Green's function) in terms of the collective modes in the charge carrier particle-hole and particle-particle channels. Following our previous discussions for the normal-state case[12], the full spin Green's function in the present pressure-induced SC state can be obtained as,

$$D(k,\omega) = D^{(0)}(k,\omega) + D^{(0)}(k,\omega)\Sigma^{(s)}(k,\omega)D(k,\omega), \quad (6)$$

then the dynamical spin structure factor of the pressure-induced two-leg ladder cuprate superconductors can be obtained explicitly in terms of full spin Green's function (6) as,

$$\begin{aligned} S(k,\omega) &= -2[1+n_B(\omega)][{\rm Im}D_L(k,\omega) + {\rm Im}D_T(k,\omega)] \\ &= -2[1+n_B(\omega)]\frac{B^2_{1k}{\rm Im}\Sigma^{(1)}_s(k,\omega)}{[\omega^2 - (\omega_{1k})^2 - B_{1k}{\rm Re}\Sigma^{(1)}_s(k,\omega)]^2 + [B_{1\mathbf{k}}{\rm Im}\Sigma^{(1)}_s(k,\omega)]^2}, \end{aligned} \quad (7)$$

where $n_B(\omega)$ is the boson distribution function, ${\rm Im}\Sigma^{(1)}_s(k,\omega) = {\rm Im}\Sigma^{(s)}_L(k,\omega) + {\rm Im}\Sigma^{(s)}_T(k,\omega)$ and ${\rm Re}\Sigma^{(1)}_s(k,\omega) = {\rm Re}\Sigma^{(s)}_L(k,\omega) + {\rm Re}\Sigma^{(s)}_T(k,\omega)$, while ${\rm Im}\Sigma^{(s)}_L(k,\omega)[{\rm Re}\Sigma^{(s)}_L(k,\omega)]$ and ${\rm Im}\Sigma^{(s)}_T(k,\omega)[{\rm Re}\Sigma^{(s)}_T(k,\omega)]$ are the corresponding imaginary (real) parts of the spin longitudinal and transverse self-energy, respectively, and this spin self-energy $\Sigma^{(s)}(k,\omega) = \Sigma^{(s)}_L(k,\omega) + \sigma_x\Sigma^{(s)}_T(k,\omega)$ with the longitudinal and transverse parts can be evaluated in terms of the charge carrier normal and anomalous Green functions in Eq. (4) and MF spin Green's function $D^{(0)}(k,\omega)$ in Eq. (5) as,

$$\Sigma^{(s)}_{L}(k,\omega) = \frac{1}{32N^2}\sum_{p,q}\sum_{\mu\nu\nu'}\Pi_{\mu\nu\nu'}(p,q,k), \tag{8a}$$

$$\Sigma^{(s)}_{T}(k,\omega) = \frac{1}{32N^2}\sum_{p,q}\sum_{\mu\nu\nu'}(-1)^{\mu+\nu+\nu'+1}\Pi_{\mu\nu\nu'}(p,q,k), \tag{8b}$$

where the kernel function,

$$\begin{aligned}\Pi_{\mu\nu\nu'}(p,q,k) &= [C_{\mu\nu'}(p-k)+C_{\mu\nu}(p+q+k)]\frac{B_{\mu k+q}}{\omega_{\mu k+q}}Z^{(\nu)}_{FA}Z^{(\nu')}_{FA}\\ &\times\left(\frac{K^{(1)}_{\mu\nu\nu'}(p,q,k)}{\omega^2-(\omega_{\mu k+q}+E_{\nu p}-E_{\nu' p+q})^2}+\frac{K^{(2)}_{\mu\nu\nu'}(p,q,k)}{\omega^2-(\omega_{\mu k+q}-E_{\nu p}+E_{\nu' p+q})^2}\right.\\ &+\left.\frac{K^{(3)}_{\mu\nu\nu'}(p,q,k)}{\omega^2-(\omega_{\mu k+q}+E_{\nu p}+E_{\nu' p+q})^2}+\frac{K^{(4)}_{\mu\nu\nu'}(p,q,k)}{\omega^2-(\omega_{\mu k+q}-E_{\nu p}-E_{\nu' p+q})^2}\right),\end{aligned} \tag{9}$$

with $C_{\mu\nu}(k)=[2t_{\parallel}\mathrm{cos}k+(-1)^{\mu+\nu}t_{\perp}]^2$, and

$$\begin{aligned}K^{(1)}_{\mu\nu\nu'}(p,q,k) &= \left(\frac{\bar{\Delta}^{(\nu)}_{hz}(p)}{E_{\nu p}}\frac{\bar{\Delta}^{(\nu')}_{hz}(p+q)}{E_{\nu' p+q}}-1-\frac{\bar{\xi}_{\nu p}}{E_{\nu p}}\frac{\bar{\xi}_{\nu' p+q}}{E_{\nu' p+q}}\right)(\omega_{\mu k+q}+E_{\nu p}-E_{\nu' p+q})\\ &\times\{n_B(\omega_{\mu k+q})[n_F(E_{\nu p})-n_F(E_{\nu' p+q})]-n_F(-E_{\nu p})n_F(E_{\nu' p+q})\},\end{aligned} \tag{10a}$$

$$\begin{aligned}K^{(2)}_{\mu\nu\nu'}(p,q,k) &= \left(\frac{\bar{\Delta}^{(\nu)}_{hz}(p)}{E_{\nu p}}\frac{\bar{\Delta}^{(\nu')}_{hz}(p+q)}{E_{\nu' p+q}}-1-\frac{\bar{\xi}_{\nu p}}{E_{\nu p}}\frac{\bar{\xi}_{\nu' p+q}}{E_{\nu' p+q}}\right)(\omega_{\mu k+q}-E_{\nu p}+E_{\nu' p+q})\\ &\times\{n_B(\omega_{\mu k+q})[n_F(E_{\nu' p+q})-n_F(E_{\nu p})]-n_F(E_{\nu p})n_F(-E_{\nu' p+q})\},\end{aligned} \tag{10b}$$

$$\begin{aligned}K^{(3)}_{\mu\nu\nu'}(p,q,k) &= \left(\frac{\bar{\Delta}^{(\nu)}_{hz}(p)}{E_{\nu p}}\frac{\bar{\Delta}^{(\nu')}_{hz}(p+q)}{E_{\nu' p+q}}+1-\frac{\bar{\xi}_{\nu p}}{E_{\nu p}}\frac{\bar{\xi}_{\nu' p+q}}{E_{\nu' p+q}}\right)(\omega_{\mu k+q}+E_{\nu p}+E_{\nu' p+q})\\ &\times\{n_B(\omega_{\mu k+q})[n_F(-E_{\nu p})-n_F(E_{\nu' p+q})]+n_F(-E_{\nu p})n_F(-E_{\nu' p+q})\},\end{aligned} \tag{10c}$$

$$\begin{aligned}K^{(4)}_{\mu\nu\nu'}(p,q,k) &= \left(\frac{\bar{\Delta}^{(\nu)}_{hz}(p)}{E_{\nu p}}\frac{\bar{\Delta}^{(\nu')}_{hz}(p+q)}{E_{\nu' p+q}}+1-\frac{\bar{\xi}_{\nu p}}{E_{\nu p}}\frac{\bar{\xi}_{\nu' p+q}}{E_{\nu' p+q}}\right)(\omega_{\mu k+q}-E_{\nu p}-E_{\nu' p+q})\\ &\times\{n_B(\omega_{\mu k+q})[n_F(E_{\nu p})+n_F(E_{\nu' p+q})-1]+n_F(E_{\nu p})n_F(E_{\nu' p+q})\},\end{aligned} \tag{10d}$$

where $n_F(\omega)$ is the fermion distribution function.

We are now ready to discuss the dynamical spin response of $Sr_{14-x}Ca_xCu_{24}O_{41}$ in the pressure-induced SC state. The dynamical spin structure factor $S(k,\omega)$ in the (k,ω) plane at the doping concentration $p=0.20$ with temperature $T=0$ for parameters $t_{\parallel}/J_{\parallel}=2.5$ and (a) $t_{\perp}/t_{\parallel}=0.4$ (underpressure) and (b) $t_{\perp}/t_{\parallel}=0.8$ (overpressure) is plotted in Fig. 2 (hereafter we use the unit of $[2\pi]$). Obviously, the mostly remarkable feature is the presence of an incommensurate-commensurate transition in the spin fluctuation geometry, where the magnetic excitation disperses with interchain coupling (then pressure). In particular, the incommensurate spin correlation in the pressure-induced SC state appears in the underpressure regime, while the commensurate spin fluctuation emerges in the overpressure regime. To check this point

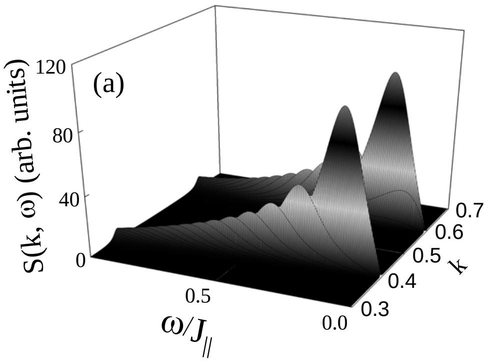

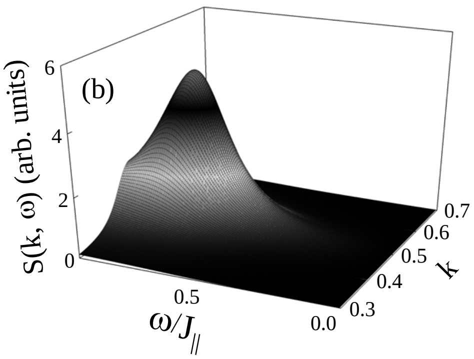

FIG. 2: The dynamical spin structure factor in the (k, ω) plane at $p = 0.20$ with $T = 0$ for $t_{\parallel}/J_{\parallel} = 2.5$ and (a) $t_{\perp}/t_{\parallel} = 0.4$ and (b) $t_{\perp}/t_{\parallel} = 0.8$.

explicitly, we plot the evolution of the magnetic scattering peaks at $p = 0.20$ in $T = 0$ for $t_{\parallel}/J_{\parallel} = 2.5$ with interchain coupling (then pressure) for $\omega = 0.4J_{\parallel}$ in Fig. 3, where there is a *critical* value (then *critical* pressure) of $t_{\perp}/t_{\parallel} \approx 0.72 = P_c$, which separates the pressure region into the underpressure ($t_{\perp}/t_{\parallel} < 0.72$) and overpressure ($t_{\perp}/t_{\parallel} > 0.72$) regimes, while $t_{\perp}/t_{\parallel} \approx 0.72$ is corresponding to the optimal pressure. In the underpressure regime $t_{\perp}/t_{\parallel} < 0.72$, the magnetic scattering peak is split into two peaks at $[1/2 \pm \delta]$ with δ as the incommensurate parameter, and is symmetric around $[1/2]$. In this case, spins are more likely to move along the legs of the ladders, rendering the materials quasi-one-dimension. However, the range of the incommensurate spin correlation decreases with increasing the strength of the interchain coupling (then pressure), and then a broad commensurate scattering peak appears in the optimal pressure and overpressure regimes $t_{\perp}/t_{\parallel} \geq 0.72$. In particular, the magnetic resonance energy is located among this broad commensurate scattering range. For determining this commensurate magnetic resonance energy in the optimal pressure, we have made a series of calculations for the intensities of the dynamical spin structure factor $S(k, \omega)$ at $p = 0.20$ with $T = 0$ for $t_{\parallel}/J_{\parallel} = 2.5$ and $t_{\perp}/t_{\parallel} = 0.72$, and the result of the intensities of $S(k, \omega)$ as a function of energy is plotted in Fig. 4, where a commensurate resonance peak centered at $\omega_r = 0.45J_{\parallel}$ is obtained. Using an reasonably estimative value[5] of $J_{\parallel} \sim 90$meV for $Sr_{14-x}Ca_xCu_{24}O_{41}$, the present result of the resonance energy in the optimal pressure is $\omega_r \approx 40.5$meV. This anticipated spin gap $\Delta_S \approx 40.5$meV is qualitatively consistent with the spin gap ≈ 32.5meV observed experimentally[5] on $Sr_{14-x}Ca_xCu_{24}O_{41}$.

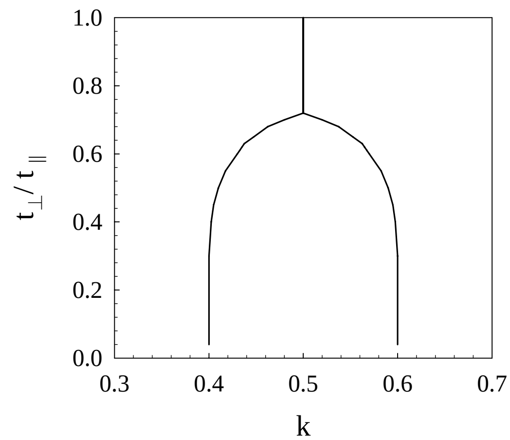

FIG. 3: The position of the magnetic scattering peaks as a function of $t_{\perp}/t_{\parallel}$ at $p = 0.20$ with $T = 0$ for $t_{\parallel}/J_{\parallel} = 2.5$ and $\omega = 0.4J_{\parallel}$.

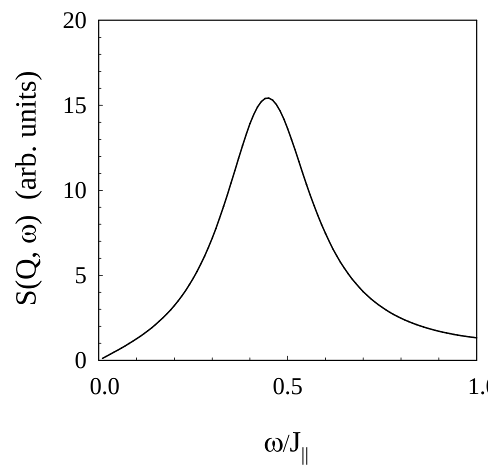

FIG. 4: The resonance energy ω_r at $p = 0.20$ with $T = 0$ for $t_{\parallel}/J_{\parallel} = 2.5$ and $t_{\perp}/t_{\parallel} = 0.72$.

In the dynamical spin response of the pressure-induced two-leg ladder cuprate superconductors, one of the characteristic features is the spin-lattice relaxation time T_1, which is closely related to the dynamical spin structure factor (7), and can be expressed as,

$$\frac{1}{T_1} = \frac{2K_BT}{g^2\mu_B^2\hbar} \lim_{\omega \to 0} \frac{1}{N} \sum_k F_{\alpha}^2(k) \frac{\chi''(k, \omega)}{\omega}, \tag{11}$$

where g is the lande-factor, μ_B is the Bohr magneton, and $F_{\alpha}(k)$ is the form factors, while the dynamical spin susceptibility $\chi''(k, \omega) = (1 - e^{-\beta\omega})S(k, \omega)$. Although

the form factors $F_\alpha(k)$ have dimension of energy, and the magnitude determined by atomic physics, and the momentum dependence determined by geometry, however, for the convenience, this form factors $F_\alpha(k)$ can be set to constant without loss of generality[12]. In Fig. 5, we plot the spin-lattice relaxation time $1/T_1$ as a function of temperature in both logarithmic scales at $p = 0.20$ for $t_\parallel/J_\parallel = 2.5$ and $t_\perp/t_\parallel = 0.7$ (underpressure), where we have chosen units $\hbar = K_B = 1$. For comparison, the corresponding experimental result[8] of $Sr_{14-x}Ca_xCu_{24}O_{41}$ at $p \approx 0.20$ is also shown in Fig. 5. The spin-lattice relaxation time T_1^{-1} shows a linear temperature dependent behavior at low temperatures ($T > T_c$) followed passes through a minimum and displays a tendency towards an increase with decreasing temperatures. In particular, it is dominated by a peak developed below the SC transition temperature T_c. Furthermore, this clear peak in T_1^{-1} also confirms that a finite SC gap exists in the quasiparticle excitation, then the spin-lattice relaxation time under the SC transition temperature decreases with decreasing temperatures, in qualitative agreement with the experimental observation on $Sr_{14-x}Ca_xCu_{24}O_{41}$[8]. In this case, this peak can be assigned to a SC coherence peak while the temperature linear dependence of T_1^{-1} at low temperatures to Korringa-type behavior. It is well-known that in the conventional metals, the temperature-linear component in T_1^{-1} in the normal state arises from paramagnetic free electrons[8]. However, in the present two-leg ladder cuprate superconductors, the interaction between charge carriers and spins from the kinetic energy term in the t-J ladder (2) induces the charge carrier-spin bound state in the normal state[12]. At low temperatures ($T > T_c$), although the most of spins in the system form the spin liquid state, the spin in the charge carrier-spin bound state moves almost freely and therefore contributes to the temperature-linear component in T_1^{-1}[12].

The essential physics of the pressure dependence of the dynamical spin response in $Sr_{14-x}Ca_xCu_{24}O_{41}$ in the pressure-induced SC state is almost the same as in the normal state case[12]. In the renormalized spin excitation spectrum $\Omega_k^2 = \omega_{1k}^2 + B_{1k}\mathrm{Re}\Sigma_s^{(1)}(k,\Omega_k)$ in Eq. (7), since both MF spin excitation spectrum ω_{1k} and spin self-energy function $\Sigma_s^{(1)}(k,\omega)$ are strong interchain coupling (then pressure) dependent, this leads to that the renormalized spin excitation spectrum Ω_k also is strong pressure dependent. Furthermore, the dynamical spin structure factor in Eq. (7) has a well-defined resonance character, where $S(k,\omega)$ exhibits peaks when the incoming neutron energy ω is equal to the renormalized spin excitation, i.e., $W(k_c,\omega) \equiv [\omega^2 - \omega_{1k_c}^2 - B_{1k_c}\mathrm{Re}\Sigma_s^{(1)}(k_c,\omega)]^2 = [\omega^2 - \Omega_{k_c}^2]^2 \sim 0$ for certain critical wave vectors $k_c = k_c^{(\mathrm{u})}$ in the underpressure regime and $k_c = k_c^{(\mathrm{o})}$ in the optimal pressure and overpressure regimes, then the weight of these peaks is dominated by the inverse of the imaginary part of the spin self-energy $1/\mathrm{Im}\Sigma^{(s)}(k_c^{(\mathrm{u})},\omega)$ in the underpressure regime and $1/\mathrm{Im}\Sigma^{(s)}(k_c^{(\mathrm{o})},\omega)$ in the optimal pressure and overpressure regimes, respectively. In particular, for the present spin self-energy $\mathrm{Re}\Sigma_s^{(1)}(k,\omega) = \mathrm{Re}\Sigma_L^{(s)}(k,\omega) + \mathrm{Re}\Sigma_T^{(s)}(k,\omega)$, $\mathrm{Re}\Sigma_L^{(s)}(k,\omega) < 0$ favors the one-dimensional behaviors, while $\mathrm{Re}\Sigma_T^{(s)}(k,\omega) > 0$ characterizes the quantum interference between the chains in the ladders, therefore there is a competition between $\mathrm{Re}\Sigma_L^{(s)}(k,\omega)$ and $\mathrm{Re}\Sigma_T^{(s)}(k,\omega)$. In the underpressure regime, the main contribution for $\mathrm{Re}\Sigma_s^{(1)}(k,\omega)$ may come from $\mathrm{Re}\Sigma_L^{(s)}(k,\omega)$, and spins and charge carriers are more likely to move along the legs, then the incommensurate spin correlation emerges, where the essential physics is almost the same as in the two-dimensional t-J model[28]. Within the CSS fermion-spin framework, as a result of self-consistent motion of charge carriers and spins, the incommensurate spin correlation is developed, which means that in the underpressure regime, the spin excitations drift away from the AF wave vector, where the physics is dominated by the spin self-energy $\mathrm{Re}\Sigma_L^{(s)}(k,\omega)$ renormalization due to charge carriers. However, the quantum interference effect between the chains manifests itself by the interchain coupling (then pressure), *i.e.*, this quantum interference increases with increasing pressure. Thus in the optimal pressure and overpressure regimes, $\mathrm{Re}\Sigma_T^{(s)}(k,\omega)$ may cancel the most incommensurate spin correlation contributions from $\mathrm{Re}\Sigma_L^{(s)}(k,\omega)$, then the commensurate spin fluctuation appears. In this sense, the pressure is a crucial role to determine the symmetry of the spin fluctuation in the two-leg ladder cuprate superconductors in the pressure-induced SC state.

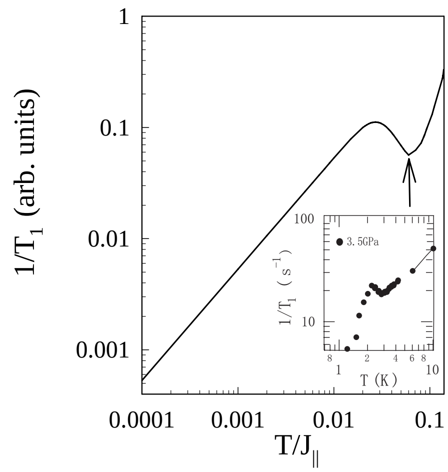

FIG. 5: The temperature dependence of the spin-lattice relaxation time $1/T_1$ in both logarithmic scales at $p = 0.20$ for $t_\parallel/J_\parallel = 2.5$ and $t_\perp/t_\parallel = 0.7$. The arrow marks the position of the superconducting transition temperature T_c. Inset: the experimental result on $Sr_{14-x}Ca_xCu_{24}O_{41}$ taken from Ref.[8].

In summary, we have shown very clearly in this paper that if the pressure effect is imitated by a variation of the

interchain coupling in the framework of the kinetic energy driven SC mechanism, the dynamical spin structure factor of the t-J ladder model calculated in terms of the collective modes in the charge carrier particle-hole and particle-particle channels per se can correctly reproduce some main features found in the NMR and NQR measurements on $Sr_{14-x}Ca_xCu_{24}O_{41}$ in the pressure-induced SC state, including the temperature dependence of the spin-lattice relaxation time, without using adjustable parameters. The theory also predicts that in the underpressure regime, the incommensurate spin correlation appears, while the commensurate spin fluctuation emerges in the optimal pressure and overpressure regimes, which should be verified by further experiments.

Acknowledgments

JQ is supported by the National Natural Science Foundation of China (NSFC) under Grant No. 11004006, YL is supported by NSFC under Grant No. 11004084, and SF is supported by NSFC under Grant No. 11074023, and the funds from the Ministry of Science and Technology of China under Grant No. 2011CB921700.

[1] Uehara Masatomo, Nagata Takashi, Akimitsu Jun, Takahashi Hiroki, Môri Nobuo and Kinoshita Kyoichi 1996 *J. Phys. Soc. Jpn.* **65** 2764

[2] Hiroi Z, Azuma M, Takano M and Bando Y 1991 *J. Solid State Chem.* **95** 230

[3] Osafune T, Motoyama N, Eisaki H and Uchida S 1997 *Phys. Rev. Lett.* **78** 1980

[4] Eccleston Roger S, Uehara Masatomo, Akimitsu Jun, Eisaki Hiroshi, Motoyama Naoki and Uchida Shin-ichi 1998 *Phys. Rev. Lett.* **81** 1702

[5] Katano S, Nagata T, Akimitsu J, Nishi M and Kakurai K 1999 *Phys. Rev. Lett.* **82** 636

[6] Isobe M, Ohta T, Onoda M, Izumi F, Nakano S, Li J Q, Matsui Y, Takayama-Muromachi E, Matsumoto T and Hayakawa H 1998 *Phys. Rev.* B **57** 613

[7] See, e.g., the review, Dagotto E 1999 *Rep. Prog. Phys.* **62** 1525, and references therein

[8] Fujiwara Naoki, Môri Nobuo, Uwatoko Yoshiya, Matsumoto Takehiko, Motoyama Naoki and Uchida Shinichi 2003 *Phys. Rev. Lett.* **90** 137001; Fujiwara N, Fujimaki Y, Uchida S, Matsubayashi K, Matsumoto T and Uwatoko Y 2009 *Phys. Rev.* B **80** 100503(R)

[9] Piskunov Y, Jérome D, Auban-Senzier P, Wzietek P and Yakubovsky A 2004 *Phys. Rev.* B **69** 014510

[10] Piskunov Y, Jérome D, Auban-Senzier P, Wzietek P and Yakubovsky A 2005 *Phys. Rev.* B **72** 064512

[11] Anderson P W 1987 *Science* **235** 1196

[12] He Jianhui, Feng Shiping and Chen Wei Yeu 2003 *Phys. Rev.* B **67** 094402

[13] Feng Shiping, Qin Jihong and Ma Tianxing 2004 *J. Phys.: Condens. Matter* **16** 343

[14] See, e.g., the review, Feng Shiping, Guo Huaiming, Lan Yu and Cheng Li 2008 *Int. J. Mod. Phys.* B **22** 3757

[15] Magishi K, Matsumoto S, Kitaoka Y, Ishida K, Asayama K, Uehara M, Nagata T and Akimitsu J 1998 *Phys. Rev.* B **57** 11533; Ohsugi S, Magishi K, Matsumoto S, Kitaoka Y, Nagata T and Akimitsu J 1999 *Phys. Rev. Lett.* **82** 4715

[16] Feng Shiping 2003 *Phys. Rev.* B **68** 184501; Feng Shiping, Ma Tianxing and Guo Huaiming 2006 *Physica* C **436** 14

[17] Qin Jihong, Chen Ting and Feng Shiping 2007 *Phys. Lett.* A **366** 611

[18] See, e.g., the review, Dagotto E and Rice T M 1996 *Science* **271** 618, and references therein

[19] Laughlin R B 1997 *Phys. Rev. Lett.* **79** 1726; Laughlin R B 1995 *J. Low. Tem. Phys.* **99** 443

[20] Feng Shiping, Su Z B and Yu L 1994 *Phys. Rev.* B **49** 2368

[21] Plakida N M 2002 *Condens. Matter Phys.* **5** 707

[22] Nagata T, Uehara M, Goto J, Akimitsu J, Motoyama N, Eisaki H, Uchida S, Takahashi H, Nakanishi T and Môri N 1998 *Phys. Rev. Lett.* **81** 1090

[23] See, e.g., Schrieffer J R *Theory of Superconductivity* (Addison-Wesley, San Francisco, 1964)

[24] Ohta Tomoko, Izumi Fujio, Onoda Mitsuko, Isobe Masaaki, Takayama-Muromachi Eiji and Hewat Alan W 1997 *J. Phys. Soc. Jpn.* **66** 3107

[25] Kato Masatsune, Shiota Kazunori and Koike Yoji 1996 *Physica* C **258** 284

[26] Qin Jihong, Yuan Feng and Feng Shiping 2006 *Phys. Lett.* A **358** 448

[27] Qin Jihong, Song Yun, Feng Shiping and Chen Wei Yeu 2002 *Phys. Rev.* B **65** 155117

[28] Feng Shiping, Ma Tianxing and Wu Xintian 2006 *Phys. Lett.* A **352** 438